

TWO-SCALE MODELLING OF REACTIVE POWDER CONCRETE BY THE METHOD OF NUMERICAL HOMOGENIZATION

A. Denisiewicz¹, M. Kuczma²

^{1,2} Institute of Building Engineering
University of Zielona Góra
ul. Licealna 9, 65-417 Zielona Góra
¹ e-mail: a.denisiewicz@ib.uz.zgora.pl
² e-mail: m.kuczma@ib.uz.zgora.pl

Keywords: numerical homogenization, reactive powder concrete, multiscale modeling, FEM.

Abstract. *The paper is concerned with the modeling of reactive powder concrete (RPC) by using the method of numerical homogenization. More specifically, we use a two-scale modeling approach and the finite element method. The behaviour of a concrete model of RPC on the macro scale is described on the basis of the phenomena occurring in the microstructure of the material. The applied approach makes it possible to design an optimal composition of the reactive powder concrete and provides the possibility to take into account the phenomena occurring in the microstructure as concerns the physical and mechanical properties of the material. The method does not require any knowledge of the constitutive equations at the macro level, which are determined implicitly for each load increment by solving a boundary value problem for the numerical model of RPC on the micro level as a representative volume element (RVE). Thus, to determine the constitutive equations on the macro scale it is necessary to know the geometry of the microstructure, the constitutive equations at the micro level and their parameters. In this contribution the material response of each material constituents (cement matrix, sand, crushed quartz) is assumed to be elastic. The microstructure of RPC concrete (RVE) is generated by a stochastic way. A computer program for two-scale homogenization has been developed and numerical results for two test problems are presented. The aim of the first two-scale test was to check the program in the case of homogeneous material. The second example present the results obtained for another micro-scale problem. Further studies of the considered problem, including also laboratory experiments, are under way.*

1 INTRODUCTION

Reactive powder concrete (RPC) is currently one of the most modern building materials produced on the basis of cement. Reactive powder concrete belongs to the class of Ultra-High Performance Concrete (UHPC) with its ultra high-strength and high ductility comparable to steel [2]. Reactive powder concretes are also classified as cement matrix composites with ultrahigh resistance properties and often called the low-temperature ceramics. Thanks to ultra high-strength and ductility of RPC concretes, the weight and dimensions of cross-sections of structures built from it can be significantly reduced, with simultaneous the large freedom in providing the structure an architectural fit and crossing over significant spans (Fig. 1).

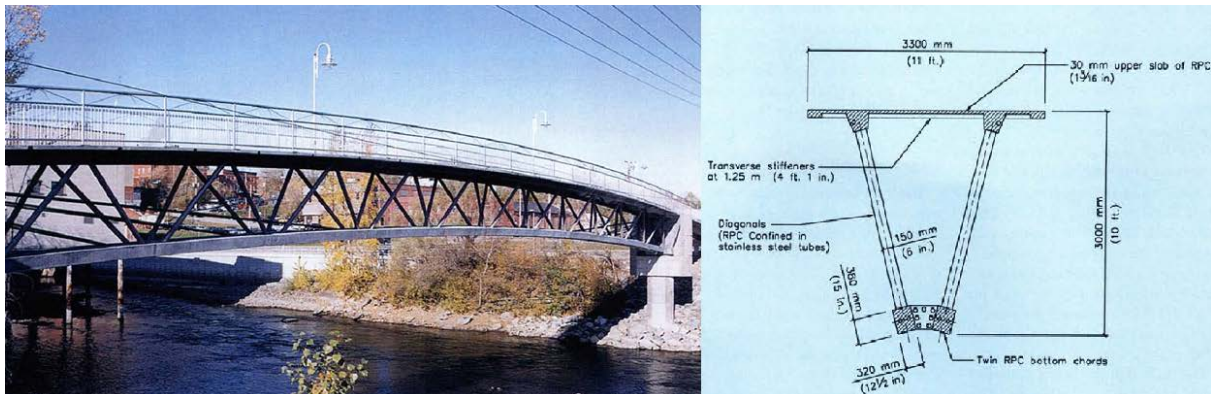


Figure 1: Pedestrian and bicycle bridge in Sherbrooke (Canada), 1997 [8]

Reactive powder concrete thanks to its physical and mechanical properties finds a wide interest not only as the construction material, but also as a cladding one and even as a material for furniture. In order to optimally design the composition of RPC concrete and for the needs of the static strength analysis of buildings and other engineering constructions made of RPC, we have developed a two-scale model of reactive powder concrete (Fig. 3) by using the numeric homogenization technique. In the method of two-scale numeric homogenization, the response of the medium on a macro-scale due to external loads is determined on the basis of structural analysis on a micro-scale. On the micro-scale level the distributions of micro-strains and micro-stresses are determined, which by the way of homogenization provide information about the macro-quantities. The whole micro-analysis is carried out on the so-called representative volumetric element (RVE). This is a volume assigned to the material point that is representative for a small surrounding of this point. When the characteristic microscopic length is one order smaller than characteristic macroscopic length, we can take into consideration only effects of the first order (Fig. 2).

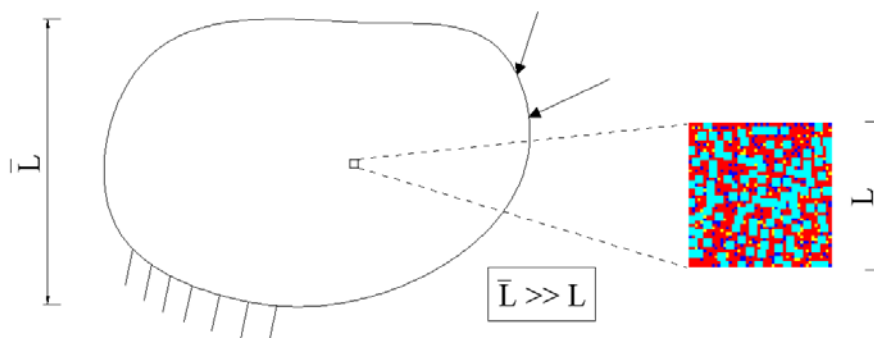


Figure 2: Assumption of high-resolution scales

In case of the RPC concrete, this condition is fulfilled. We may assume that the characteristic dimension on micro-scale is a fraction of ground quartz, 0.2 mm. While on the macro-scale this will be the dimension of the cross-section of a structural element, e.g. 0.2 x 0.2 m.

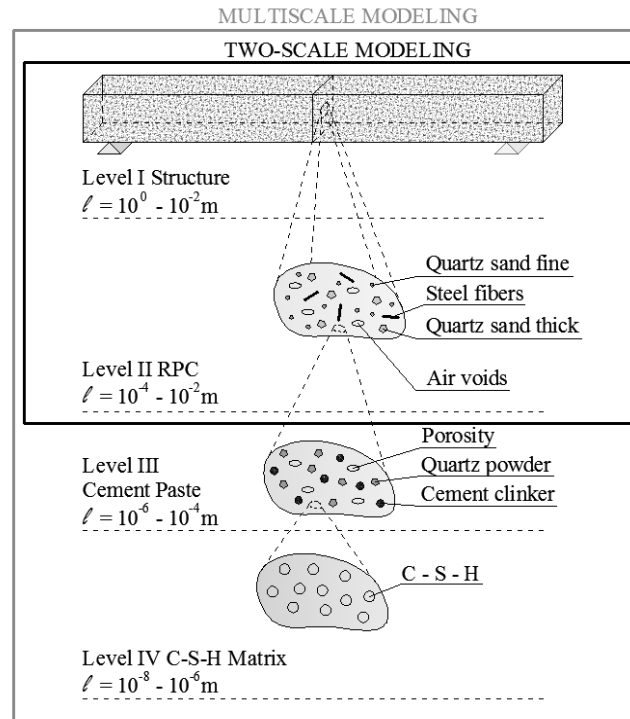


Figure 3: Level analysis

2 MICROSTRUCTURE OF RPC AND REPRESENTATIVE VOLUME ELEMENT

Reactive powder concrete (RPC) is manufactured by elimination of the shortcomings of the traditional concrete, and especially by minimizing porosity to the level of about 4% by:

- using aggregates with granulation enabling the maximal packaging of components,
- potentially maximal reduction of the water-cement ratio, with simultaneous application of super-plasticizers,
- applying treatments of pressing in the initial period of cementitious binding.

The improvement of physical and mechanical properties can also be obtained by modifying the microstructure of the adhesive matrix by using the right thermal treatment and through using admixtures of very small grains, e.g., ground fine quartz and silica fume. Contrary to traditional concrete, where the aggregate constitutes the reinforcing element but usually a chemically passive component, the micro-aggregate in RPC concrete exhibit the pozzolanic activity. The main characteristic features of the RPC microstructure are [7]:

- very compact microstructure of the C-S-H phase,
- very good adhesion of the C-S-H phase to mineral inclusions in the form of powder grains and quartz sand and steel fibers.

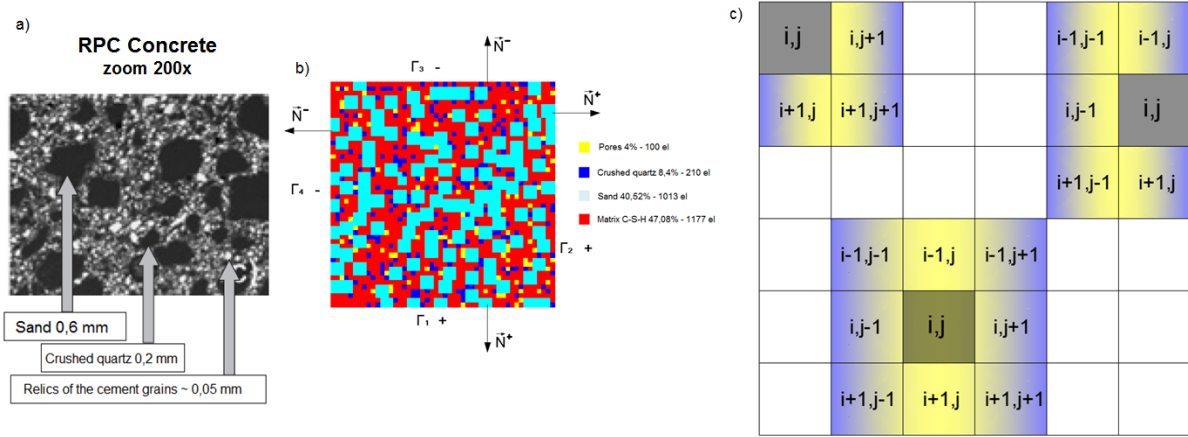


Figure 4: Representative volume element: a) microstructure of RPC, b) RVE, c) scheme of planting FE elements with RVE constituents

In order to model the microstructure of RPC concrete with the composition given in Table 1, as the first approximation we have applied a two-dimensional representative volume element. The RVE is modeled with the help of the finite element method. The RVE is a square and consists of 2500 finite elements, each of dimensions 0.2 x 0.2 mm; the side of RVE is 10 mm in length and consists of 50 finite elements. Because of the random character of the arrangement of concrete's components, we have utilized a stochastic method to generate the RVE structure (Fig. 4b).

Component	Volume [kg/m ³]	Percentage [%]
Cement	705	28,20
Silica fume	230	9,20
Crushed quartz	210	8,40
Sand	1013	40,52
Superplasticizer	17	0,68
Steel fibers	140	5,60
Water	185	7,40

Table 1. Composition of RPC concrete

Building the RVE structure consists in the random selection of an element (from the 50x50 grid) and also the random assignment of the component (pores, crushed quartz, sand, cement matrix) to the selected position. The basic component length was assumed equal to 0.2 mm. In the case of drawing the sand component, the process of arranging elements of the grid takes place according to the scheme presented in Fig. 4c, which is connected with the maximal size of the grain equal to 0.6 mm. The boundary locations correspond to the smaller grains of the same component. In order to generate a natural pseudo-random number γ_{n+1} from the range $\langle 1, 4 \rangle$ for a component and the one from $\langle 1, 50 \rangle$ for the component's position, a generator defined by the following formula was applied

$$\gamma_{n+1} = \text{int}[x + (y - x + 1) \cdot X_{n+1}] \quad (1)$$

in which x is the left end of the range of drawing and y is the right end of the range of drawing

$$\begin{aligned}
X_{n+1} &= (aX_n + b) \bmod c \\
a &= 7^5 = 16807 \quad b = 0 \\
c &= 2^{31} - 1 = 2147483647
\end{aligned}
\tag{2}$$

It is an affine generator of pseudo-random numbers from the $\langle 0, 1 \rangle$ range. The whole procedure of building the structure of the represented volume element is performed by our own computer program written in the FORTRAN 90 language, in which open access libraries [9,10] were used. The issue of approximation of the random microstructures is discussed in depth in [6].

3 TWO-SCALE COMPUTATIONAL HOMOGENIZATION

3.1 Homogenization

The idea of two-scale computational homogenization is illustrated in Fig. 5.

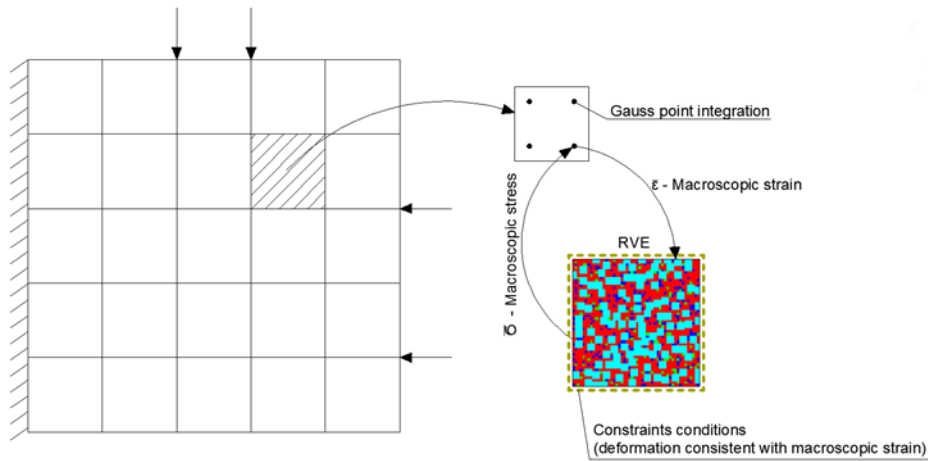


Figure 5: Idea of two-scale computational homogenization

The problem of homogenization over the RVE of volume V is to find a displacement field $\mathbf{u}(X)$ such that $div[\boldsymbol{\sigma}] = \mathbf{0}$ in V , while satisfying the boundary conditions on Γ so that the Hill energy criterion is fulfilled:

$$\bar{\boldsymbol{\sigma}} \cdot \bar{\boldsymbol{\varepsilon}} = \langle \boldsymbol{\sigma} \cdot \boldsymbol{\varepsilon} \rangle
\tag{3}$$

where the bar over a quantity says that it is a macroscopic quantity and the notation is used:

$$\langle \bullet \rangle \stackrel{df}{=} \frac{1}{V} \int_V \bullet dV
\tag{4}$$

3.2 Finite element method in computational homogenization

For solving the problem on the macro and the micro scales, the displacement version of the finite element method was used. The domains of both the problems are discretized with four-node finite element Q4 that has two degrees of freedom at each node (Fig. 7), which are the

nodal values of the horizontal $u = u(\xi, \eta)$ and vertical $v = v(\xi, \eta)$ components of the displacement field $\mathbf{u} = (u, v)$, and bilinear shape functions N_1, \dots, N_4 shown in Fig. 6:

$$\begin{aligned} N_1(\xi, \eta) &= \frac{1}{4}(1 - \xi - \eta + \xi\eta) & N_2(\xi, \eta) &= \frac{1}{4}(1 + \xi - \eta - \xi\eta) \\ N_3(\xi, \eta) &= \frac{1}{4}(1 + \xi + \eta + \xi\eta) & N_4(\xi, \eta) &= \frac{1}{4}(1 - \xi + \eta - \xi\eta) \end{aligned} \quad (5)$$

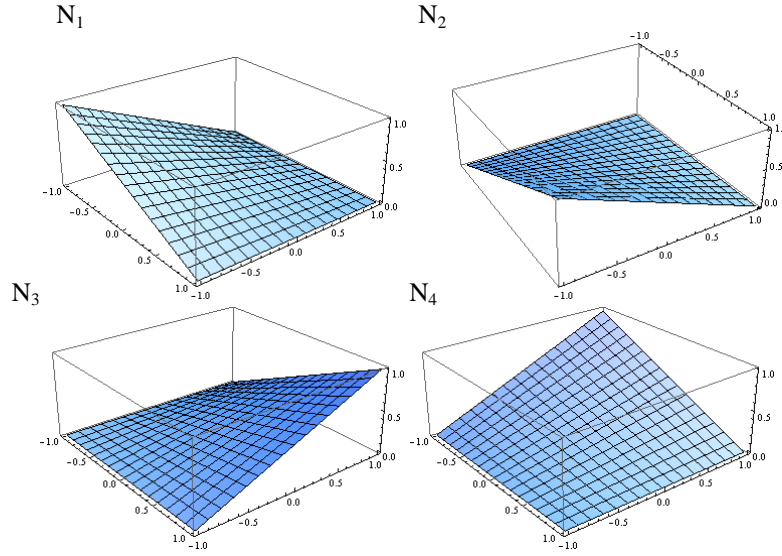


Figure 6. Bilinear shape functions

The relationship between the components of deformation and displacement of nodes in the plane state of stress is expressed in matrix form by the formula

$$\boldsymbol{\varepsilon} = \begin{bmatrix} \varepsilon_{11} \\ \varepsilon_{22} \\ 2\varepsilon_{12} \end{bmatrix} = \partial \mathbf{N} \mathbf{q} = \mathbf{B} \mathbf{q} \quad (6)$$

where ∂ is the matrix operator of partial derivatives, \mathbf{B} is the matrix of deformations including the derivatives of shape functions and $\mathbf{q}^T = [u_1, v_1, u_2, v_2, u_3, v_3, u_4, v_4]$ is the vector of nodal displacements of the finite element. The displacement field within the finite element $\Omega_e \subset \Omega$ is defined by

$$\mathbf{u} = \mathbf{N} \mathbf{q} \quad (7)$$

where

$$\mathbf{N} = \begin{bmatrix} N_1 & 0 & N_2 & 0 & N_3 & 0 & N_4 & 0 \\ 0 & N_1 & 0 & N_2 & 0 & N_3 & 0 & N_4 \end{bmatrix} \quad (8)$$

Each material component of the microstructure is modeled as a linear elastic isotropic material. For the isotropic material and the considered plane stress state, the stiffness matrix is expressed by the formula

$$\mathbf{K}^e = \int_{\Omega_e} \mathbf{B}^T \mathbf{D}_i \mathbf{B} d\Omega \quad (9)$$

where

$$\mathbf{D}_i = \frac{E_i}{1-\nu_i^2} \begin{bmatrix} 1 & \nu_i & 0 \\ \nu_i & 1 & 0 \\ 0 & 0 & \frac{1-\nu_i}{2} \end{bmatrix} \quad (10)$$

and $i = 1, 2, 3$ is the number of a particular component of the microstructure.

Finally, the system of algebraic FEM equations on macro-scale can be written in the form

$$\bar{\mathbf{K}} \bar{\mathbf{u}} = \bar{\mathbf{F}} \quad (11)$$

in which $\bar{\mathbf{K}}$ is the global macro-scale stiffness matrix,

$$\bar{\mathbf{K}} = \mathbf{A} \int_{\Omega^E} \mathbf{B}^T \bar{\mathbf{C}} \mathbf{B} d\Omega \quad (12)$$

where the symbol \mathbf{A} stands for the aggregation procedure of macro-scale finite elements E contributions and $\bar{\mathbf{C}}$ is the tangent stiffness matrix, which will be discussed below in Section 3.4.

3.3 The boundary value problem on micro-scale

The boundary value problem of mechanics for the specified RVE after FEM discretization is solved by the minimization of the function with additional constraints

$$\min_{\mathbf{u}} \varphi(\mathbf{u}) = \frac{1}{2} \mathbf{u}^T \mathbf{K} \mathbf{u} - \mathbf{u}^T \mathbf{f} \quad s.t. \quad \mathbf{C} \mathbf{u} - \mathbf{g} = \mathbf{0} \quad (13)$$

The BVP can be solved by using the Lagrange's method, but for the method of numeric homogenization we have a large computational complexity, that's why the approach based on Lagrange's multipliers is too time consuming. Because of that, there was selected an alternative approach [1, 3], which brings down to the solution of the equations:

$$\tilde{\mathbf{K}} \mathbf{u} = \tilde{\mathbf{F}} \quad (14)$$

where

$$\tilde{\mathbf{K}} = \mathbf{A} \left[(\mathbf{C}_u^e)^T \mathbf{C}_u^e + (\mathbf{Q}_u^e)^T \mathbf{K}^e \mathbf{Q}_u^e \right] \quad (15)$$

$$\tilde{\mathbf{F}} = \mathbf{A} \left[\mathbf{D}_u^e \bar{\mathbf{e}} [(\mathbf{C}_u^e)^T - (\mathbf{Q}_u^e)^T \mathbf{K}^e \mathbf{R}_u^e] \right] \quad (16)$$

$$\mathbf{Q}_u^e = \mathbf{I} - \mathbf{R}_u^e \mathbf{C}_u^e \quad (17)$$

$$\mathbf{R}_u^e = (\mathbf{C}_u^e)^T [(\mathbf{C}_u^e \mathbf{C}_u^e)^T]^{-1} \quad (18)$$

To enforce deformations of RVE in accordance with macro-deformations $\bar{\mathbf{e}}$ there were applied the displacement boundary conditions of the first type [3,4,5]:

$$\mathbf{C}_u^e \mathbf{u} = \mathbf{D}_u^e \bar{\boldsymbol{\varepsilon}} = \mathbf{g}_u^e \quad (19)$$

where

$$\mathbf{C}_u^e = \int_{\Gamma} \mathbf{H}_u \mathbf{N}^T \mathbf{N} d\Gamma \quad (20)$$

$$\mathbf{D}_u^e = \int_{\Gamma} \mathbf{H}_u \mathbf{N}^T \mathbf{X} d\Gamma \quad (21)$$

and the matrix \mathbf{H}_u , in the case of displacement boundary conditions that we have applied in this paper, is equal to the 8x8 unit matrix.

The finite element Q4 used in the analysis, definition of boundary Γ and the way of integrating are presented in Fig. 7 and Eqn. (27).

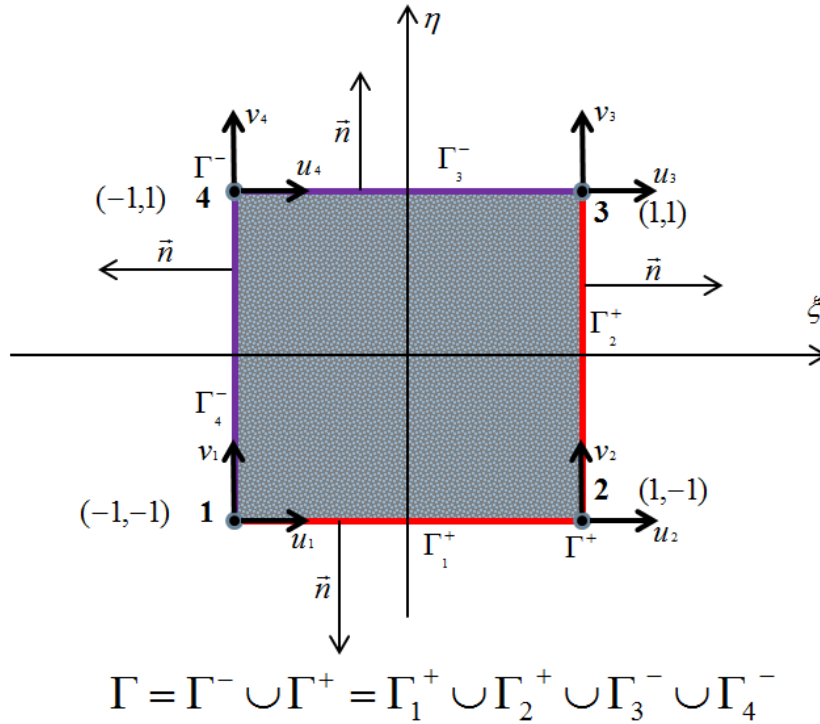


Figure 7: Finite element Q4 – single element RVE

The representative volume element (RVE) in micro-scale is a representation of the material point in macro-scale. Let \mathbf{x} be the position vector of a point on the edge Γ , then

$$\mathbf{x}_{\Gamma_2^+} = \mathbf{x}_{\Gamma_4^-} + \mathbf{x}_2 - \mathbf{x}_1 = \mathbf{x}_{\Gamma_4^-} + \Delta \mathbf{x} \quad (22)$$

and using the assumption that the RVE is a point we have

$$\lim_{\Delta \mathbf{x} \rightarrow \mathbf{0}} (\mathbf{x}_{\Gamma_4^-} + \Delta \mathbf{x}) = \mathbf{x}_{\Gamma_4^-} \quad (23)$$

$$\mathbf{x}_{\Gamma_2^+} = \mathbf{x}_{\Gamma_4^-} \quad (24)$$

Analogously on the top and bottom edges,

$$\mathbf{x}_{\Gamma_1^+} = \mathbf{x}_{\Gamma_3^-} + \mathbf{x}_4 - \mathbf{x}_1 = \mathbf{x}_{\Gamma_3^-} + \Delta \mathbf{x} \quad (25)$$

$$\mathbf{x}_{\Gamma_1^+} = \mathbf{x}_{\Gamma_3^-} \quad (26)$$

Thus

$$\begin{aligned} \int_{\Gamma} (\bullet)(\xi, \eta) d\Gamma &= \int_{-1}^1 (\bullet)(\xi, -1) d\xi + \int_{-1}^1 (\bullet)(1, \eta) d\eta \\ &+ \int_{-1}^1 (\bullet)(\xi, 1) d\xi + \int_{-1}^1 (\bullet)(-1, \eta) d\eta \end{aligned} \quad (27)$$

3.4 Macrostress and tangent stiffness matrix

We determine the macro-stress $\bar{\boldsymbol{\sigma}}$ and the tangent stiffness matrix $\bar{\mathbf{C}}$ in the macro-scale problem by solving the three linear systems of equations (14) for the RVE [3]:

$$\begin{aligned} \delta \bar{\boldsymbol{\sigma}}^1 &\text{ for } \delta \bar{\boldsymbol{\varepsilon}} = [1, 0, 0] \\ \delta \bar{\boldsymbol{\sigma}}^2 &\text{ for } \delta \bar{\boldsymbol{\varepsilon}} = [0, 1, 0] \\ \delta \bar{\boldsymbol{\sigma}}^3 &\text{ for } \delta \bar{\boldsymbol{\varepsilon}} = [0, 0, 1] \end{aligned} \quad (28)$$

$$\bar{\mathbf{C}} = [\delta \bar{\boldsymbol{\sigma}}^1 \quad \delta \bar{\boldsymbol{\sigma}}^2 \quad \delta \bar{\boldsymbol{\sigma}}^3] ; \quad \bar{\mathbf{C}} = \begin{bmatrix} \delta \bar{\sigma}_{11}^1 & \delta \bar{\sigma}_{11}^2 & \delta \bar{\sigma}_{11}^3 \\ \delta \bar{\sigma}_{22}^1 & \delta \bar{\sigma}_{22}^2 & \delta \bar{\sigma}_{22}^3 \\ \delta \bar{\sigma}_{12}^1 & \delta \bar{\sigma}_{12}^2 & \delta \bar{\sigma}_{12}^3 \end{bmatrix} \quad (29)$$

and

$$\bar{\boldsymbol{\sigma}} = \frac{1}{V} \sum_e (\mathbf{D}_u^e)^T \boldsymbol{\lambda}^e \quad (30)$$

where

$$\boldsymbol{\lambda}^e = (\mathbf{R}_u^e)^T (\mathbf{F}^e - \mathbf{K}^e \mathbf{u}^e) \quad (31)$$

$\mathbf{u}^e \equiv \mathbf{q} = [u_1, v_1, u_2, v_2, u_3, v_3, u_4, v_4]^T$ is a vector of nodal micro-displacements in RVE, $\mathbf{F}^e = \mathbf{0}$ is a vector of nodal micro-loads in RVE (herein assumed zero).

4 NUMERICAL EXAMPLES

We begin with a basic test on a single element homogenous RVE, on which the unit macro-deformations, e.g. $\bar{\varepsilon}_{11} = 1$, $\bar{\varepsilon}_{22} = 0$, $\bar{\varepsilon}_{12} = 0$, as shown in Figs. 8 and 9 were enforced. The calculated deformed shapes of the RVE are displayed as bright colour lines. The next test serves as a check of our two-scale analysis computer program. In Figs. 10 and 11 the obtained numerical results in a two-scale analysis of the homogeneous disc under compression in the plane state stress are presented. The homogeneous microstructure is modelled by a square 5x5 RVE with elasticity parameters given in Fig. 10. The results obtained in a two-scale analysis by our

program written in FORTRAN 90 are compared with those by using the commercial program ABAQUS. The next test concerns the microstructure of 50x50 RVE (top of Fig. 12), which was generated randomly by (1) and contains: cement matrix (47.08%), sand (40.52%), crushed quartz (8.40%), pores (4%). The assumed values of elasticity parameters are: cement matrix – $E = 30$ GPa, $\nu = 0.16$, crushed quartz and sand – $E = 75$ GPa, $\nu = 0.3$. The boundary value problem induced by the macro-strain $\bar{\epsilon} = [-1, 0, 0]$ on the RVE was solved. The distributions of micro-stresses σ_{11} and σ_{22} are shown in Fig. 12a,b.

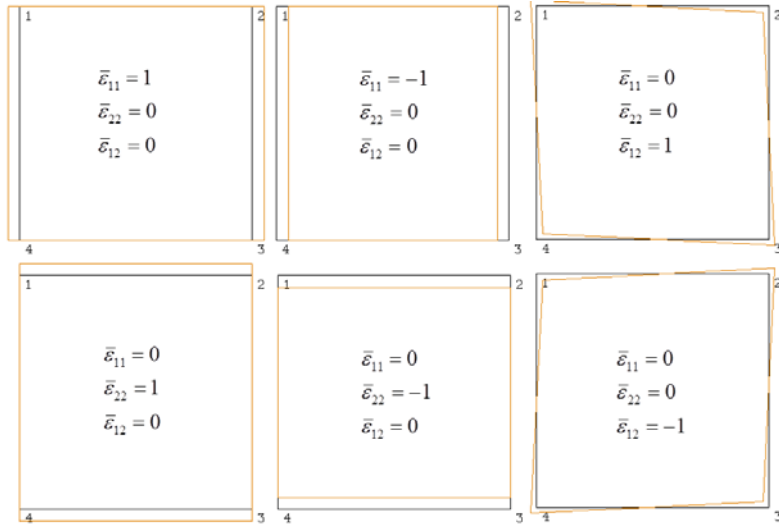


Figure 8: Tests on single-element cell

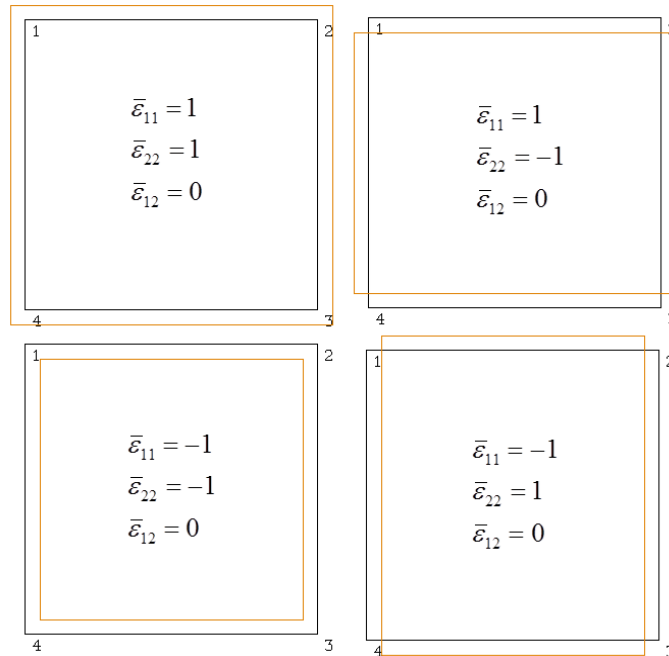


Figure 9: Tests on single-element cell

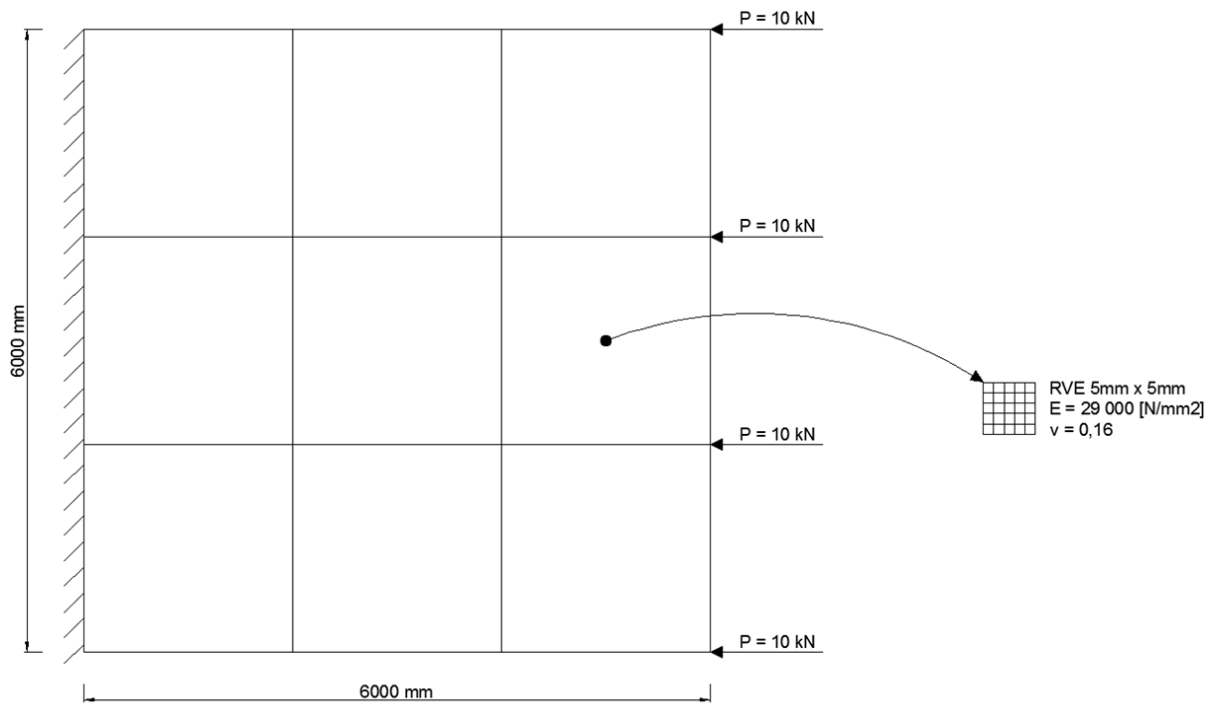


Figure 10: Two-scale analysis for a homogenous material

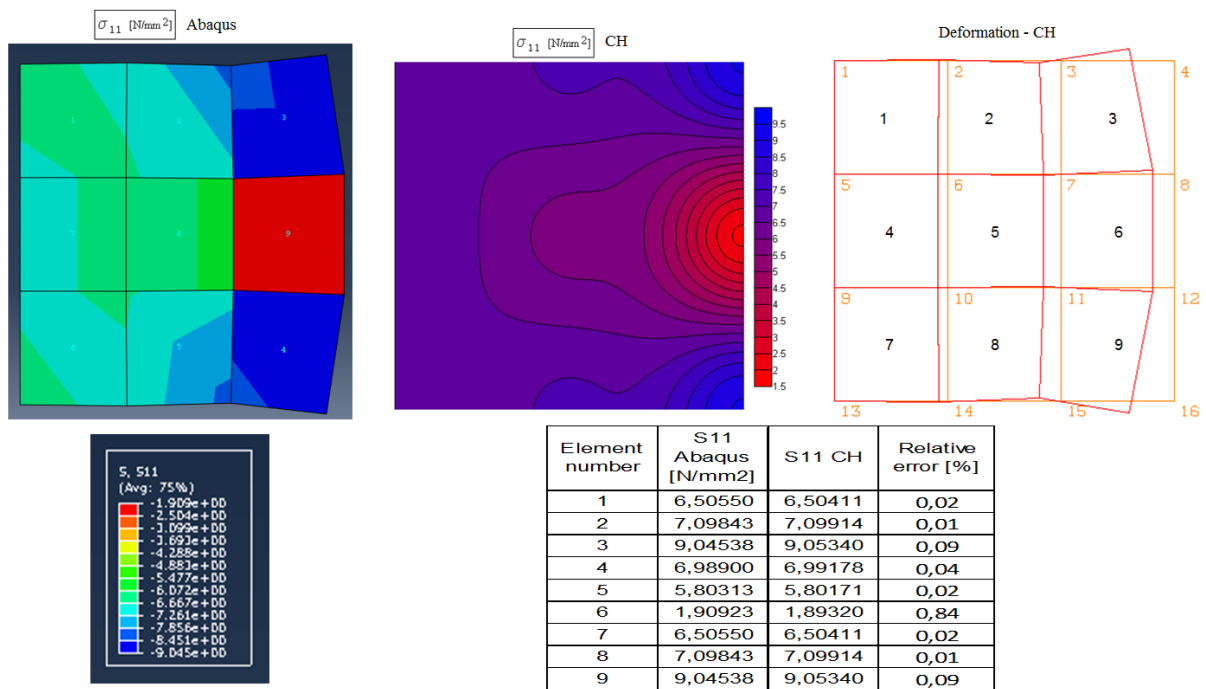


Figure 11: Comparison of the results obtained in two-scale analysis (CH) by our own computer program and of that by ABAQUS for a homogenous material

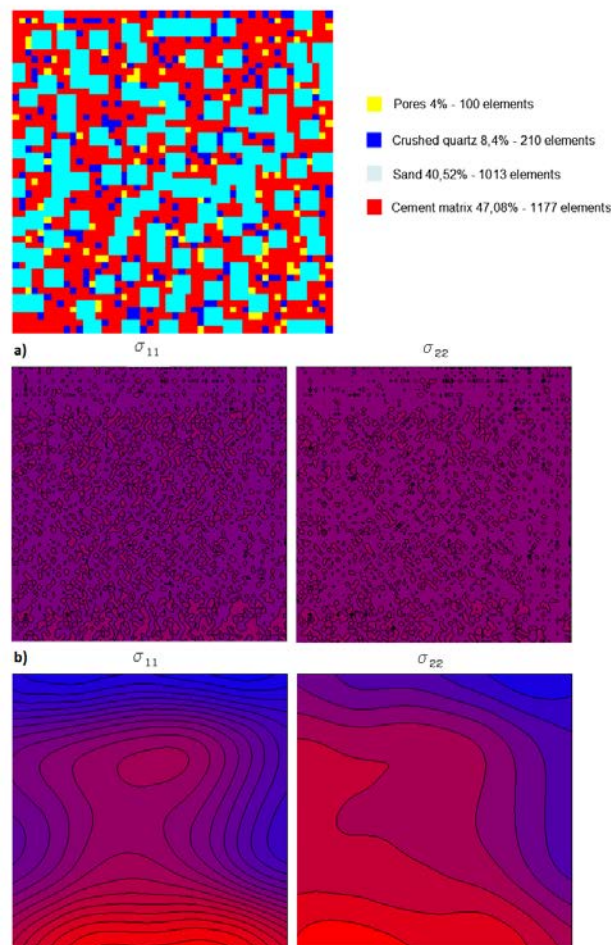


Figure 12: Microstructure of the RVE, a) micro-stress distributions, b) smoothed micro-stress distributions

ADDITIONAL INFORMATION

Article was prepared as part of a research grant 506-07-01-03 MNiSW.

REFERENCES

- [1] M. Ainsworth: Essential boundary conditions and multi-point constraints in finite element analysis, *Comput. Methods Appl. Mech. Engrg.* 190, (2001) 6323 - 6339.
- [2] J. Jasiczak, A. Wdowska, T. Rudnicki: Ultra-High Performance Concretes. Properties, technology, applications (in Polish). Association of Cement Producers (Stowarzyszenie Producentów Cementu), Kraków 2008.
- [3] Ł. Kaczmarczyk: Numerical analysis of selected problems in the mechanics of inhomogeneous media (in Polish). PhD thesis. Cracow University of Technology 2006.
- [4] V.G. Kouznetsova, M.G.D. Geers, W.A.M. Brekelmans: Multi-scale second-order computational homogenization of multi-phase materials: a nested finite element solution strategy. *Comput. Methods Appl. Mech. Engrg.* 193, (2004) 5525 - 5550.

- [5] C. Miehe: Computational micro-to-macro transitions for discretized micro-structures of heterogeneous materials at finite strains based on the minimization of averaged incremental energy. *Comput. Methods Appl. Mech. Engrg.* 192, (2003) 559 - 591.
- [6] J. Schröder, D. Balzani, D. Brands: Approximation of random microstructures by periodic statistically similar representative volume elements based on lineal-path functions. *Arch Appl Mech* 81 (2011) 975–997.
- [7] T. Zdeb, J. Śliwiński: Reactive powder concrete – mechanical properties and microstructure (in Polish). *Budownictwo Technologie Architektura* 51, (2010) 51 - 55.
- [8] P. Y. Blais, M. Couture, Precast, Prestressed Pedestrian Bridge – World’s First Reactive Powder Concrete Structure. *PCI Jurnal* May-June 1999.
- [9] DISLIN Scientific Plotting Software <http://www.mps.mpg.de/dislin/>
- [10] SLATEC A Mathematical Library <http://www.netlib.org/slatec/index.html>